

MOMENT-ROTATION CHARACTERISTICS OF LOCALLY BUCKLING BEAMS

By

M. IVÁNYI

Department of Steel Structures, Technical University, Budapest
(Received: November 30, 1978)

1. Introduction

A necessary (but not sufficient) condition of the development of unrestricted yielding of a structure is to have the moment bearing capacity of the beam (cross sections) characterized partly by the ultimate moment value, and partly by the ability of the beam to support this ultimate moment up to an adequate plastic hinge rotation. Also the possibility of a premature plate buckling or lateral buckling disturbing the moment bearing capacity of the beam unit has to be considered. The plate buckling is affected by the plate proportions and the supporting effect of adjacent plate parts. The lateral buckling is affected by the slenderness of sections between lateral supports.

In the following, the problem how the moment-rotation relationship of the beam section is affected by plate buckling, by other words, the determination of the yield mechanism curve due to buckling of constituent plates will be considered.

2. Previous research

HAAIJER, G. and THÜRLIMANN, B. [1] investigated the plate slenderness of webs of beams in bending sufficient to permit adequate deformation capacity. Their analyses were based on the discontinuous character of the yielding of steel, taking the effect of residual stresses into consideration. HAAIJER and THÜRLIMANN investigated separately the effects of flange and web buckling, with regard to the supporting effect of "adjacent" plate parts. Nevertheless, the effect of interaction between the buckling plate parts upon the entire cross section, however intensive it might be, was ignored. Test results support the assumption that buckling of plates of I-sections under bending moments do not develop independently but are geometrically compatible (Fig. 1). Thereby interdependent buckling of plates constituting the entire cross section is to be reckoned with by determining the moment-rotation relationship of the beam cross section.

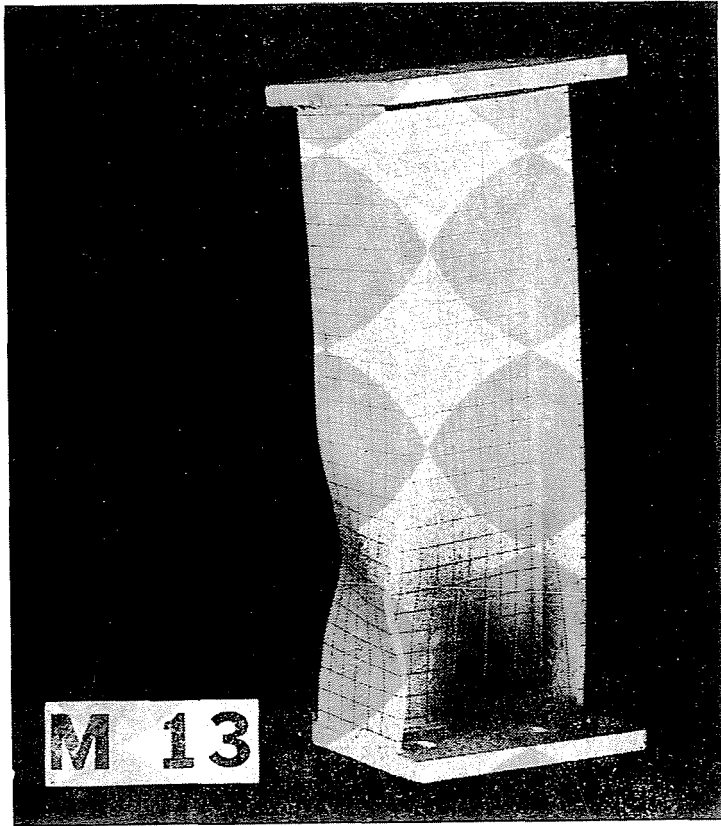


Fig. 1. Flange buckling of specimen M-13

3. Yield mechanism curves for beams under uniform moment

The kinematic theorem of plasticity will be applied, giving an upper bound. A total yield mechanism will be selected, so as to possibly correspond to geometrical conditions and to the assumed yield criterion.

This method has been applied by CLIMENHAGA, J. J. and JOHNSON, R. [2] for a special case, i.e. the effect of plate buckling in the steel component of composite beams at supports. For the basic assumptions and a simple example of the behaviour of a plastic hinge due to bending moment, we refer to [3].

For determining the yield mechanism curve due to the buckling of plates constituting a beam (flanges and web) — taking test results into consideration — the yield mechanism in Fig. 2 will be selected.

In the shaded area, plastic deformation develops, while thick lines are linear plastic hinges behaving as described in [3]. Moment M produces tensile and compressive zones. In the tensile zone, plastic deformation develops in the

flange section EF, and in zone AEF of the web plate. In the compressive zone, plastic deformation develops in the zone BCD of the web, and plastic hinges AB, AC, AD, BD and CD arise. Also, plastic deformations develop in zone GHJK of the compression flange, with the development of plastic hinges MK, KQ, NH, HP and GK, GH, JK, JH.

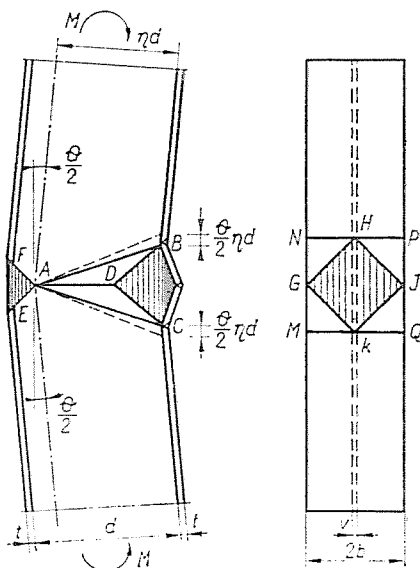


Fig. 2

The yield mechanism in the compressive zone of the web is compatible with that in the compression flange if points B and H, as well as C and K coincide. Thereby the yield mechanism of the entire section becomes determinate, save the position of point A, assumed at a distance $\eta \cdot d$.

Now, strain and potential energies can be written for the yield mechanisms of each plate part. (Strain energy of yield mechanisms of plate parts will be presented in the Appendix.)

According to the analyses:

$$\int_{\theta} M \cdot d\theta = W = W_{EF} + W_{AEF} + W_{BCD} + W_{AD} + 2W_{AB} + 2W_{BD} + W_{KJ} + 4W_{NH} + W_{GG} + W_{BC} \quad (1)$$

Moment M will be determined by deriving (1):

$$M = \frac{dW}{d\theta} = \frac{dW_{EF}}{d\theta} + \frac{dW_{AEF}}{d\theta} + \frac{dW_{BCD}}{d\theta} + \frac{dW_{AD}}{d\theta} + 2 \frac{dW_{AB}}{d\theta} + 2 \frac{dW_{BD}}{d\theta} + \frac{dW_{KJ}}{d\theta} + 4 \frac{dW_{NH}}{d\theta} + \frac{dW_{GG}}{d\theta} + \frac{dW_{BC}}{d\theta} \quad (2)$$

(Also values of the yield mechanisms $\frac{dW}{d\theta}$ for each plate part are shown in the Appendix.)

Eq. (2) can be made dimensionless by introducing the ultimate moment of the I-section:

$$M_P = 2 \left[bt(d+t) \sigma_{Yf} + \frac{d^2}{8} v \sigma_{Yw} \right] \quad (3)$$

with the corresponding elastic rotation

$$\theta_Y = \frac{M_P L}{2E J_x} \quad (4)$$

where

$$J_x = \frac{vd^3}{12} + [bt(d+t)^2] + \frac{bt^3}{3} \quad (5)$$

hence:

$$\frac{M}{M_P} = \frac{1}{M_P} \cdot \frac{dW}{d\theta} \quad (6)$$

In the knowledge of geometry data and material characteristics, assuming different θ and θ/θ_Y values, the M and M/M_P values can be determined to obtain the yield mechanism curve of the beam.

σ_{Yw} and σ_{Yf} will be assumed to be yield points of web and flange, respectively, with E_S as strain-hardening modulus for both.

These analyses involve several approximations: so the assumed stress-strain relation is valid for a small deformation only. Rotation of the plastic hinge has to be limited [2], unless plastic hinges assumed in Fig. 3a are replaced by those according to Fig. 3b. It would, however, make the analysis of the assumed model much more difficult, while other approximations and test results fail to justify this refinement.

Reduction of the plastic hinge moment due to simultaneous compressive force has been omitted, and so has been the secondary effect due to the spatiality of the yield mechanism.

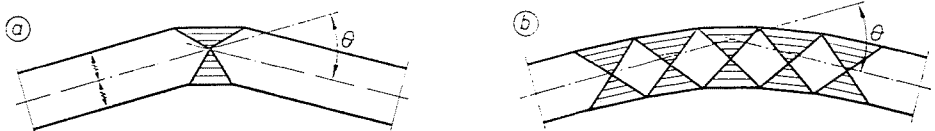


Fig. 3

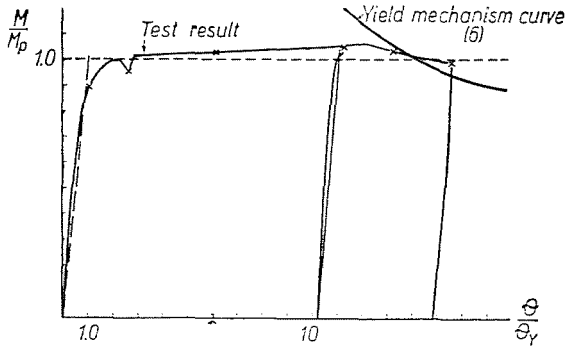


Fig. 4. Specimen M-13; $d = 200$ mm, $v = 4$ mm, $2b = 120$ mm, $t = 8$ mm, $L = 580$ mm, $\sigma_{yw} = 26$ Mp/mm², (260 MPa) $\sigma_{yf} = 29$ Mp/mm², (290 MPa) $E_s = 9.2$ Mp/mm², (92 MPa) $d/v = 50$, $2b/t = 15$

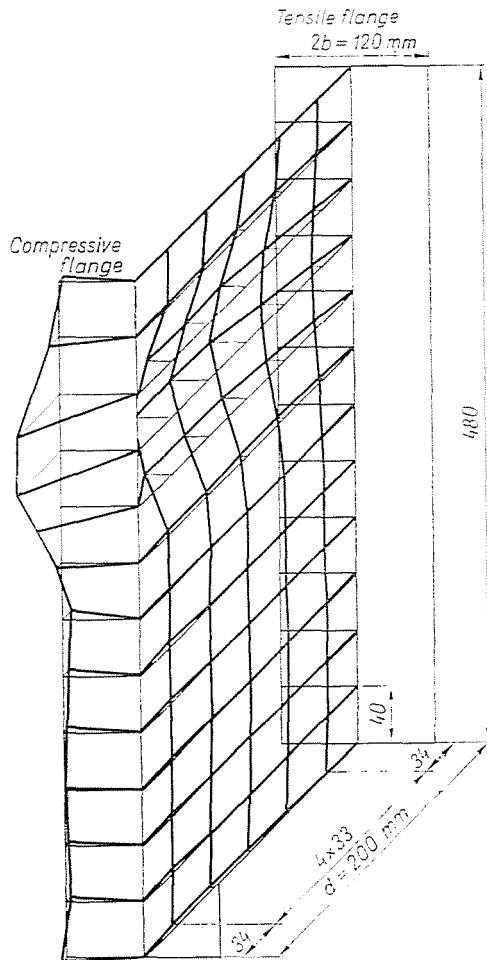


Fig. 5. Specimen M-13. No deformations due to bending have been plotted

This analysis is not concerned with the minimization of the $M-\theta$ relationship with respect to η , nevertheless the specimen to be presented in Chapter 4 exhibited — assuming different η values — a minimum of $M-\theta$ for $\eta = 0.83$. The $M-\theta$ relationship has been plotted in Fig. 4.

Validity of the approximations in determining the yield mechanism curve, of rather simple treatment, has been confirmed by test results.

4. Experimental verification

In 1977, a theoretical and experimental program has been established at the Department of Steel Structures, for investigating plastic plate buckling [4].

From among results of tests on specimens, those for No. $M-13$ will be presented, with dimensionless $M-\theta$ relationship and test results shown in Fig. 4. Buckled web and flange configurations are seen in Fig. 5.

Test results confirm that the web and flange buckling — for given plate proportions — are not independent geometrically.

Summary

The yield mechanism curve is a means to analyze the effect of buckling of plates constituting the cross section of beams, permitting to select the proportions of the constituting plates to make up a structure with the deformation capacity needed for a favourable plastic behaviour, of importance for the plastic design of steel structures.

References

1. HAAIJER, G.—THÜRLIMANN, B.: On Inelastic Buckling in Steel, J. of the Eng. Mech. Division, ASCE Vol. 84, EM2, April, 1958.
2. CLIMENHAGA, J. J.—JOHNSON, R.: Moment-Rotation Curves for Locally Buckling I-Beams and Composite Beams. University of Cambridge, Technical Report CUED/C-Struct/TR20 Sept. 1971.
3. IVÁNYI, M.: Yield-Mechanism Curves Due to Local Buckling of Axially Compressed Members. Periodica Polytechnica, C. E. Vol. 23 (1979) No. 3—4.
4. IVÁNYI, M.: Limits of Plate Slenderness in Plastic Design. Final Report; Regional Colloquium on Stability of Steel Structures, Hungary, 1977.

Appendix

Strain energies of yield mechanisms of plate parts are:

A.1. Tensile section (Figs A1, A2)

A.1.1. Plastic zone in the tensile flange:

Axial flange strains along section EF:

$$\varepsilon = \frac{1}{2} \left(\frac{\theta}{2} + \frac{\theta}{2} \right) = \frac{1}{2} \theta. \quad (\text{A1})$$

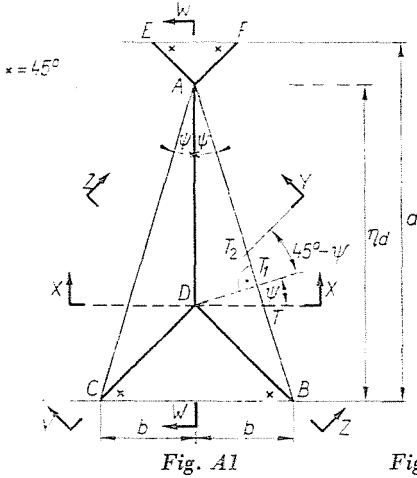


Fig. A1

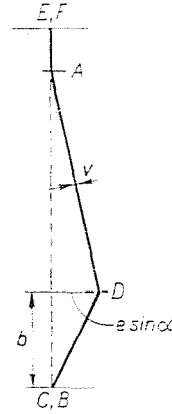


Fig. A2. Section W-W

Utilizing rigid-strain-hardening material characteristics, the deformation energy becomes:

$$W_{EF} = V_{EF} \int_0^{\theta/2} (\sigma_{YF} + \epsilon \cdot E_s) d\epsilon = 2bt[2(1 - \eta)d + t] \left\{ \sigma_{YF} + \frac{\theta \cdot E_s}{4} \right\} \frac{\theta}{2}. \quad (A2)$$

Differentiating:

$$\frac{dW_{EF}}{d\theta} = bt[2(1 - \eta)d + t] \left\{ \sigma_{YF} + \frac{\theta \cdot E_s}{2} \right\}. \quad (A3)$$

A.1.2. Plastic zone in the tensile web zone:

Axial strains (A1):
Strain energy:

$$W_{AEF} = V_{AEF} \int_0^{\theta/2} (\sigma_{Yw} + \epsilon \cdot E_s) d\epsilon = v(1 - \eta)^2 d^2 \left\{ \sigma_{Yw} + \frac{\theta \cdot E_s}{4} \right\} \frac{\theta}{2}. \quad (A4)$$

Differentiating:

$$\frac{dW_{AEF}}{d\theta} = v(1 - \eta)^2 d^2 \left\{ \sigma_{Yw} + \frac{\theta \cdot E_s}{2} \right\} \frac{1}{2}. \quad (A5)$$

A.2. Compressive web zone

A.2.1. Plastic zone BCD

Axial strains in the zone BCD are:

$$\epsilon = \frac{\theta \eta d}{2b}. \quad (A6)$$

Strain energy:

$$W_{BCD} = vb^2 \int_0^{\theta \eta d / 2b} (\sigma_{Yw} + \epsilon \cdot E_s) d\epsilon = vb \left\{ \sigma_{Yw} + \frac{\eta d \theta E_s}{4b} \right\} \frac{\theta \eta d}{2}. \quad (A7)$$

Deriving:

$$\frac{dW_{BCD}}{d\theta} = \frac{1}{2} vb \eta d \left\{ \sigma_{Yw} + \frac{\eta d \cdot \theta \cdot E_s}{2b} \right\}. \quad (A8)$$

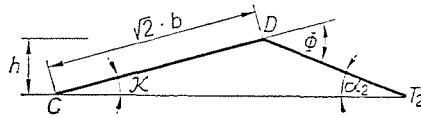


Fig. A4. Section Y-Y

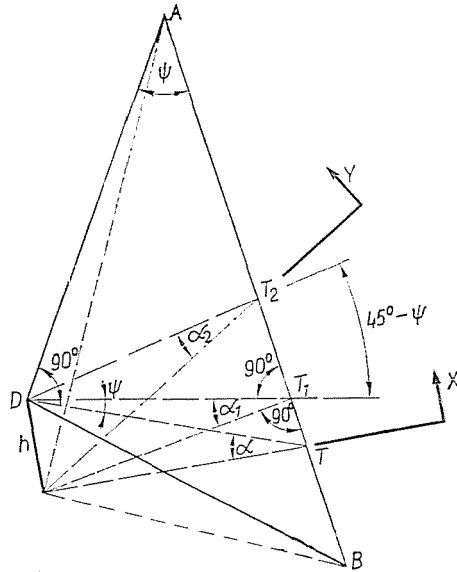


Fig. A5. $\overline{TD} = e$; $\overline{T_1D} = e_1$; $\overline{T_2D} = e_2$

A.2.3. Plastic hinges AB and AC

Rotation α_1 of plastic hinge AB can be determined according to Figs A4 and A5. According to Fig. A5, for $DT = e$ and $DT_1 = e_1$:

$$\sin \alpha = \frac{h}{e} \tag{A21}$$

$$\sin \alpha_1 = \frac{h}{e_1} \tag{A22}$$

$$\cos \psi = \frac{e_1}{e} = \frac{\sin \alpha}{\sin \alpha_1} \tag{A23}$$

$$\sin \alpha_1 = \frac{\sin \alpha}{\cos \psi} \tag{A24}$$

$$\alpha_1 = \arcsin \left\{ \frac{\sin \alpha}{\cos \psi} \right\} . \tag{A25}$$

Obviously:

$$\operatorname{tg} \psi = \frac{\sin \psi}{\cos \psi} = \sqrt{\frac{1}{\cos^2 \psi} - 1} ; \quad \cos \psi = \frac{1}{\sqrt{1 + \operatorname{tg}^2 \psi}} .$$

Needing derivative of α_1 with respect to θ :

$$\frac{d\alpha_1}{d\theta} = \frac{1}{\sqrt{1 - \sin^2 \alpha_1}} \cdot \frac{1}{\cos \psi} \cdot \frac{\cos \alpha}{\sin \alpha} \cdot \frac{\eta d}{2b}. \quad (\text{A26})$$

Plastic hinge strain:

$$\varepsilon = \frac{\alpha_1}{2}. \quad (\text{A27})$$

Strain energy being:

$$\bar{W}_{AB} = \int_0^{\alpha_1/2} (\sigma_{Yw} + \varepsilon \cdot E_s) d\varepsilon = \frac{v^2 \cdot \eta d}{2 \cos \psi} \left\{ \sigma_{Yw} + \frac{\alpha_1 \cdot E_s}{4} \right\} \frac{\alpha_1}{2}. \quad (\text{A28})$$

The derivative with respect to θ , utilizing (A26):

$$\frac{d\bar{W}_{AB}}{d\theta} = v^2 \eta d \left\{ \sigma_{Yw} + \frac{\alpha_1 E_s}{2} \right\} \left\{ \frac{d\alpha_1}{d\theta} \right\} \frac{1}{4 \cos \psi} = \frac{d\bar{W}_{AC}}{d\theta}. \quad (\text{A29})$$

A.2.4. Plastic hinges *BD* and *CD*

Rotation of plastic hinge *BD* may be determined from the section *Y-Y* in Fig. A1, normal to the hinge line.

Rotation of hinge *BD*:

$$\bar{\phi} = \varkappa + \alpha_2 \quad (\text{A30})$$

$$\sin \varkappa = \frac{h}{\sqrt{2} \cdot b} \quad (\text{A31})$$

The h value from section *X-X* (Fig. A3):

$$h = e \cdot \sin \alpha \quad (\text{A32})$$

$$\varkappa = \arcsin \left\{ \frac{e \cdot \sin \alpha}{\sqrt{2} b} \right\}. \quad (\text{A33})$$

From Fig. A4, $DT_2 = e_2$, and from Fig. A5:

$$\cos(45^\circ - \psi) = \frac{e_1}{e_2} \quad (\text{A34})$$

considering that

$$\cos(45^\circ - \psi) = \frac{\sqrt{2}}{2} \cos \psi (1 + \operatorname{tg} \psi) \quad (\text{A35})$$

and

$$\cos \psi = \frac{e_1}{e} \quad (\text{A36})$$

we obtain:

$$\sin \alpha_2 = \frac{h}{e_2} = \frac{e \cdot \sin \alpha \cdot \cos(45^\circ - \psi)}{e_1} = \frac{\sqrt{2}}{2} (1 + \operatorname{tg} \psi) \cdot \sin \alpha \quad (\text{A37})$$

$$\alpha_2 = \arcsin \left(\frac{\sqrt{2}}{2} (1 + \operatorname{tg} \psi) \sin \alpha \right). \quad (\text{A38})$$

Needing the derivative of $\sin \alpha$ with respect to θ :

$$\frac{d(\sin \alpha)}{d\theta} = \frac{\cos \alpha}{\sin \alpha} \frac{\eta d}{2b} \tag{A39}$$

and the derivative of Φ with respect to θ , utilizing (A33), (A38) and (A39):

$$\frac{d\Phi}{d\theta} = \left[\frac{1}{\sqrt{1 - \sin^2 \alpha}} \frac{e}{\sqrt{2} b} + \frac{1}{\sqrt{1 - \sin^2 \alpha_2}} \frac{\sqrt{2}}{2} (1 + \operatorname{tg} \psi) \right] \left(\frac{\eta d}{2b} \right) \frac{\cos \alpha}{\sin \alpha} \tag{A40}$$

Plastic hinge strain:

$$\varepsilon = \frac{\Phi}{2} \tag{A41}$$

$$W_{BD} = V_{BD} \int_0^{\phi/2} (\sigma_{Yw} + \varepsilon E_s) d\varepsilon = \frac{\sqrt{2}}{2} b v^2 \left\{ \sigma_{Yw} + \frac{\Phi \cdot E_s}{4} \right\} \frac{\Phi}{2} . \tag{A42}$$

Derivative with respect to θ , utilizing (A40):

$$\frac{dW_{BD}}{d\theta} = \frac{\sqrt{2}}{4} b v^2 \left\{ \sigma_{Yw} + \frac{\Phi \cdot E_s}{2} \right\} \left\{ \frac{d\Phi}{d\theta} \right\} = \frac{dW_{CD}}{d\theta} . \tag{A43}$$

A.3. Compression flange (Fig. A6)

A.3.1. Plastic zone KGHJ

Strain:

$$\varepsilon = \frac{\eta d}{2b} \theta . \tag{A44}$$

Strain energy:

$$W_{KJ} = V_{KJ} \int_0^{\eta d/2b \theta} (\sigma_{Yf} + \varepsilon \cdot E_s) d\varepsilon - b t \eta d \left\{ \sigma_{Yf} + \frac{\theta \cdot \eta d \cdot E_s}{4b} \right\} \theta . \tag{A45}$$

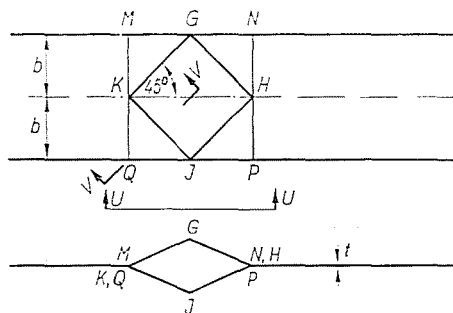


Fig. A6

Differentiating:

$$\frac{dW_{KJ}}{d\theta} = b\eta d \left\{ \sigma_{Yf} + \frac{\theta \eta d E_s}{2b} \right\}. \quad (\text{A46})$$

A.3.2. Plastic hinges NH, NP, QK and KM

Section U—U in Fig. A6 is seen in Fig. A7 showing plastic hinge rotations:

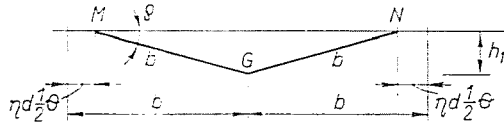


Fig. A7. Section M—N

$$h_1 = \sqrt{b^2 - \left(b - \frac{\eta d \theta}{2}\right)^2} = \sqrt{b \cdot \eta d \cdot \theta - \frac{(\eta d \theta)^2}{4}} \quad (\text{A47})$$

$$\sin \varrho = \frac{h_1}{b} \quad (\text{A48})$$

$$\varrho = \arcsin \left\{ \frac{\sqrt{b \eta d \theta - (\eta d \theta)^2 \frac{1}{4}}}{b} \right\} \quad (\text{A49})$$

Needing derivative of ϱ with respect to θ :

$$\frac{d\varrho}{d\theta} = \frac{1}{\cos \varrho} \cdot \frac{1}{2b} \frac{b \eta d - \eta d \cdot \theta \frac{1}{2}}{\sqrt{b \cdot \eta d \cdot \theta - (\eta d \cdot \theta)^2 \frac{1}{4}}}. \quad (\text{A50})$$

Strain in the plastic hinge:

$$\varepsilon = \frac{\varrho}{2} \quad (\text{A51})$$

$$W_{NH} = V_{NH} \int_0^{\varrho/2} (\sigma_{Yf} + \varepsilon \cdot E_s) d\varepsilon = 2bt^2 \left\{ \sigma_{Yf} + \frac{\varrho E_s}{4} \right\} \frac{\varrho}{2}. \quad (\text{A52})$$

Derivative with respect to σ , utilizing (A50):

$$\frac{dW_{NH}}{d\theta} = bt^2 \left\{ \sigma_{Yf} + \frac{\varrho E_s}{2} \right\} \left\{ \frac{d\varrho}{d\theta} \right\} = \frac{dW_{HP}}{d\theta} = \frac{dW_{QK}}{d\theta} = \frac{dW_{KM}}{d\theta}. \quad (\text{A53})$$

A.3.3. Plastic hinges GH, HJ, JK and KG

Section V—V in Fig. A6 is seen in Fig. A8 showing a plastic hinge rotation 2λ . From geometry causes:

$$h_2 = \frac{h_1}{2}. \quad (\text{A54})$$

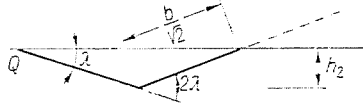


Fig. A8. Section V—V

Utilizing (A48):

$$\sin \lambda = \frac{\sqrt{2} h_2}{b} = \frac{\sqrt{2}}{2} \sin \varrho \tag{A55}$$

$$\lambda = \arcsin \left\{ \frac{\sqrt{2}}{2} \sin \varrho \right\}. \tag{A56}$$

Needing derivative of λ with respect to θ , utilizing (A50):

$$\frac{d\lambda}{d\theta} = \frac{1}{\cos \lambda} \cdot \frac{\sqrt{2}}{2} \cdot \cos \varrho \left\{ \frac{d\varrho}{d\theta} \right\}. \tag{A57}$$

Plastic hinge strain:

$$\varepsilon = \frac{2\lambda}{2} = \lambda. \tag{A58}$$

Strain energy for the four hinges:

$$W_{GG} = V_{GG} \int_0^\lambda (\sigma_{Yf} + \varepsilon E_s) d\varepsilon = 2 \sqrt{2} b t^2 \left\{ \sigma_{Yf} + \frac{\lambda \cdot E_s}{2} \right\} \lambda. \tag{A59}$$

Derivative with respect to θ , utilizing (A57):

$$\frac{dW_{GG}}{d\theta} = 2 \sqrt{2} b t^2 \left\{ \sigma_{Yf} + \frac{\lambda \cdot E_s}{2} \right\} \left\{ \frac{d\lambda}{d\theta} \right\}. \tag{A60}$$

A.4. Plastic hinge BC

Plastic hinge between the web and the flange — assumed in the web — is seen in Fig. A9
 Plastic hinge rotation:

$$\omega = \varrho - \arcsin \left\{ e \frac{\sin \alpha}{b} \right\}. \tag{A61}$$

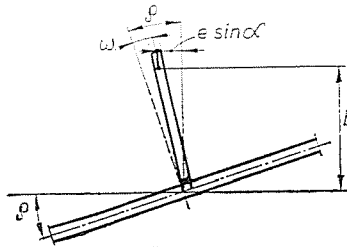


Fig. A9

Needing derivative with respect to θ , utilizing (A50):

$$\frac{d\omega}{d\theta} = \frac{d\varrho}{d\theta} - \frac{1}{\sqrt{1 - \left(\frac{e \sin \alpha}{b} \right)^2}} \cdot \frac{e}{b} \cdot \frac{\cos \alpha}{\sin \alpha} \cdot \frac{\eta d}{2b}. \tag{A62}$$

Plastic hinge strain:

$$\varepsilon = \frac{\omega}{2}. \quad (\text{A63})$$

Strain energy:

$$W_{BC} = V_{BC} \int_0^{\omega/2} (\sigma_{Yf} + \varepsilon \cdot E_s) d\varepsilon = v^2 b \left\{ \sigma_{Yf} + \frac{\omega \cdot E_s}{4} \right\} \frac{\omega}{2}. \quad (\text{A64})$$

Derivative with respect to θ :

$$\frac{dW_{BC}}{d\theta} = \frac{v^2 b}{2} \left\{ \sigma_{Yf} + \frac{\omega E_s}{2} \right\} \left\{ \frac{d\omega}{d\theta} \right\}. \quad \text{A65)}$$

Associate Prof. Dr. Miklós IVÁNYI, H-1521, Budapest